Journal of Applied Physics ARTICLE pubs.aip.org/aip/jap

A thermodynamic theory of coupling between point-defect diffusion and dislocation plasticity

Cite as: J. Appl. Phys. **137**, 155901 (2025); doi: 10.1063/5.0257553
Submitted: 10 January 2025 · Accepted: 26 March 2025 ·
Published Online: 15 April 2025

View Online Export Citation CrossMark

Charles K. C. Lieou[1,a)] and Brian D. Wirth[1,2]

AFFILIATIONS

[1]Department of Nuclear Engineering, University of Tennessee, Knoxville, Tennessee 37996, USA
[2]Fusion Energy Group, Oak Ridge National Laboratory, Oak Ridge, Tennessee 37830, USA

[a)]**Author to whom correspondence should be addressed:** clieou@utk.edu

ABSTRACT

This article describes a unified, thermodynamically consistent model for irradiation creep that combines dislocation glide and the stress-induced preferential absorption (SIPA) of point defects at dislocations. Central to the model is the premise that the dynamics of point defects, such as interstitials and vacancies, is controlled by temperature, while the dynamics of extended defects, among which dislocations are of prime relevance, is controlled by an effective temperature that pertains to the configurational degrees of freedom that evolve on a much slower time scale than the kinetic-vibrational degrees of freedom and, as such, fall out of equilibrium with the former. Results for thermal and irradiation creep in copper and aluminum suggest that conventional SIPA mechanisms are inadequate to explain the pronounced dependence of the irradiation creep rates on stress and temperature, necessitating nontrivial corrections to the SIPA dislocation climb rates. These results provide important insights into the stress and temperature dependencies of dislocation climb.

I. INTRODUCTION

Irradiation creep is a ubiquitous phenomenon in crystalline metals and is of practical interest to the nuclear materials community. At stresses below yielding and moderate-to-high homologous temperatures, it is known to be driven by the diffusion of interstitial atoms and vacancies whose creation is enhanced by neutron or ion bombardment. In nuclear reactors, irradiation creep has significant implications for the irreversible deformation and lifetimes of reactor components. Despite the importance of this phenomenon, the modeling and simulation of creep behavior remains a major challenge.

Various models for creep have been proposed in the literature.[1–8] The review paper by Matthews and Finnis[9] provides a comprehensive survey of irradiation creep models. Many of these models are largely empirical in character, relying on power-law fits to the stress; and distinct models may, in fact, describe phenomena or mechanisms under somewhat different conditions that share the same underlying origin. Among models concerned with the microscopic origins of diffusional creep, the class of stress-induced preferential absorption (SIPA) models, first proposed by Refs. 10–13 and more recently reviewed in Ref. 14, is among the most widely accepted in the literature. The basic idea is that the stress configuration establishes orientational anisotropy within the material, which causes the preferential diffusion of vacancies and interstitials, as well as the enhanced absorption of these point defects at sinks oriented in preferred directions. In particular, the absorption of point defects at dislocations results in dislocation climb, which produces plastic strain. More recent investigations of SIPA-type mechanisms include Ref. 15, which proposed a discrete stochastic model for the interaction between point defects and dislocations, established the importance of stress gradients in vacancy diffusion, and predicted significantly increased dislocation climb velocities than in older literature, as well as Ref. 16, which identified the existence of a hydrostatic stress minimum around dislocation loops which traps vacancies, contrary to the belief that vacancy absorption at dislocations amounts to the immediate annihilation of the former.

However, the SIPA model itself does not deal with the diffusional strain arising from the kinematics and dynamics of point defects alone independently of the presence of sinks, a process that operates even in the absence of irradiation or external stresses. To this end, it is necessary to augment SIPA with a physics-based model. One such notable attempt was made by Berdichevsky *et al.*,[17]

where they were able to derive, using the laws of thermodynamics, the equilibrium concentrations of interstitials and vacancies, alongside equations for their temporal evolution. Their work, however, had a major conceptual error in that there is no such thing as plastic displacement. Villani *et al.*[18] further refined their work, which provides the basis for the recent treatment in Chakraborty *et al.*[19] in which the statistical thermodynamics of vacancies were combined with essential ingredients of the SIPA model to simulate the diffusion and absorption of vacancies at dislocations and grain boundaries. However, Ref. 19 neglected interstitials and, more importantly, did not treat dislocations on the same footing as vacancies, as if dislocations would not contribute to the energy and entropy of the material and need not obey the same laws of thermodynamics that govern the temporal evolution of their density. Other authors (e.g., Refs. 20–24) have argued, within the Thermodynamic Dislocation Theory (TDT), that the energy and entropy of the dislocations must be taken into account in order to develop a thermodynamically consistent model of dislocation glide and explain phenomena in which heat exchange plays an important role.

In the present work, we seek to fill this gap by combining SIPA and the thermodynamically consistent description of point-defect diffusion as elucidated in Refs. 17–19 with TDT[20–24] to establish a unified multiphysics model for creep arising from point-defect diffusion, dislocation climb, and dislocation glide. While the dynamics of point defects is controlled by temperature, corresponding to the kinetic-vibrational degrees of freedom, we follow TDT and argue that the dynamics of extended defects such as dislocations is controlled by an effective temperature associated with the configurational degrees of freedom, or the mechanically stable positions of constituent atoms. In addition, we restrict ourselves to polycrystal aggregates in which the random orientations of grains suggest that an isotropic theory—without the need to simulate various crystal orientations or resolve distinct slip systems—should suffice, despite the fact that the applied stress sets up spatial anisotropy.

This paper is organized as follows. In Sec. II, we elucidate the framework of statistical thermodynamics that lays the groundwork for the remainder of the paper. Then, in Sec. III, we follow Ref. 18 and propose an expression for the diffusional strain rate and use the machinery of statistical thermodynamics to derive important constraints on the dynamics of vacancies and interstitials. Next, in Sec. IV, we develop expressions for the plastic strain rates associated with dislocation glide according to TDT and dislocation climb according to SIPA, summarizing all evolution equations in Sec. VI. In Sec. VI, we compare model results and experiments described in Ref. 25 for irradiation and thermal creep of copper and aluminum and suggest that the conventional SIPA expression for the irradiation creep rate must be modified in both cases with a thermal activation term containing a stress barrier to account for the pronounced stress and temperature dependence of the steady-state creep rate. We conclude the paper in Sec. VII with a summary of our findings as well as suggestions for future work.

II. INTERNAL VARIABLES AND STATISTICAL THERMODYNAMICS

In this section and in Secs. III and IV, we describe the proposed creep processes included in the model, which are mediated by a coupling between dislocation plasticity and the diffusion of vacancies and interstitials. This is largely based on the work of Chakraborty *et al.*,[19] which, in turn, is based on Refs. 17 and 18. However, Ref. 19 neglects interstitials and appears to have errors with the deviatoric part of the strain rate due to the flow of point defects, as well as the physical dimensions of some quantities. In addition, that work did not deal with the thermodynamics of dislocations, which are known to contribute to the configurational energy and entropy.[20] The present attempt is an improvement in those aspects.

We start by defining our internal state variables that represent the density of defects. These include the number of point defects of type α per unit volume, c^α, where $\alpha = I, V$ for interstitials and vacancies, as well as the density of extended defects of type β, ρ_β. These may include, for example, dislocations on different slip systems indexed by β as well as grain boundaries. In the case of dislocations, the corresponding density variable ρ_D refers to the length of dislocation lines per unit volume. In anticipation that we are dealing with a polycrystal, we neglect the distinction between slip systems and use a single scalar dislocation density ρ_D. We also neglect the grain-boundary density, or the area of grain boundaries per unit volume, in what follows, but shall keep the superscript β for bookkeeping purposes.

It is convenient to use dimensionless internal state variables in place of dimensional ones. To this end, we replace c^α by

$$\eta^\alpha \equiv \Omega_0 c^\alpha, \quad \alpha = I, V, \tag{1}$$

where Ω_0 is the atomic volume. Meanwhile, instead of ρ_D, the length of dislocation lines per unit volume, we use the dimensionless dislocation density

$$\rho \equiv a^2 \rho_D, \tag{2}$$

where $a \sim 10b$ represents the minimum separation between dislocations, with b being the length of the Burgers vector, such that $\Omega_0 \sim b^3$. This can be easily extended to describe dislocations on different slip systems β, in which case ρ^β now refers to the dimensionless dislocation densities.

The densities of point defects obey the simple continuity equation

$$\dot{\eta}^\alpha = -\nabla \cdot \mathbf{j}^\alpha + f^\alpha; \quad \alpha = I, V, \tag{3}$$

where $\mathbf{j}^\alpha$ is the flux of point defects of class α and f^α is the production rate, both in appropriate units so that η is dimensionless.

Point defects, namely, interstitials and vacancies, can be created by thermal excitation alone, however low their concentration may be. The same cannot be said about extended defects such as dislocations and grain boundaries; these correspond to a separate, slower set of configurational degrees of freedom, plausibly controlled by a different temperature, that is weakly coupled to the kinetic-vibrational degrees of freedom of the constituent atoms. With this in mind, we separate the energy and entropy per unit volume, U and S, into kinetic-vibrational and configurational

contributions, denoted by the subscripts K and C, and write

$$U = U_K + U_C; \quad S = S_K + S_C. \tag{4}$$

Roughly speaking, U_C and S_C are attributed to the mechanically stable positions of the constituent atoms—thus, one may regard U_C as arising from the interatomic potential energy—while U_K and S_K are associated with the thermal motion of the atoms about their mechanically stable positions. This leads to the definition of temperature θ and the effective temperature χ (in energy units), respectively, as

$$\theta = \left(\frac{\partial U_K}{\partial S_K}\right)_{\eta^\alpha}; \quad \chi = \left(\frac{\partial U_C}{\partial S_C}\right)_{\rho^\beta}. \tag{5}$$

Using the differential chain rule, the time derivatives of the thermal and configurational energy densities can now be written as

$$\dot{U}_K = \theta \dot{S}_K + \sum_\alpha \left(\frac{\partial U_K}{\partial \eta^\alpha}\right)_{S_K} \dot{\eta}^\alpha - p\frac{\dot{V}^{\mathrm{el}}}{V}, \tag{6}$$

$$\dot{U}_C = \chi \dot{S}_C + \sum_\beta \left(\frac{\partial U_C}{\partial \rho^\beta}\right)_{S_C} \dot{\rho}^\beta + \frac{\partial U_C}{\partial t}. \tag{7}$$

In Eq. (6), p is the hydrostatic pressure, V is the extensive volume, and $\dot{V}^{\mathrm{el}}$ is the rate of reversible, elastic volumetric expansion or contraction.

According to the first law of thermodynamics, the total energy density changes at a rate that is equal to the work rate per unit volume, minus the energy lost by conduction and convection with the surroundings. Thus,

$$\dot{U} = \dot{U}_C + \dot{U}_K = \sigma_{ij}\dot{\varepsilon}_{ij} - \nabla\cdot\mathbf{q}_K - \nabla\cdot\mathbf{q}_C - A(\theta-\theta_0). \tag{8}$$

In Eq. (8), σ_{ij} and $\dot{\varepsilon}_{ij}$ are the stress and total strain rate tensors. $\mathbf{q}_K = -K_K\nabla\theta$ and $\mathbf{q}_C = -K_C\nabla\chi$ are the rates of heat and effective heat conduction, which follow from Fourier's law, with K_K and K_C being the non-negative conductivities. θ_0 is the ambient temperature, so that $A(\theta-\theta_0)$ with $A \geq 0$ is the rate at which heat is lost to the surroundings. It will be useful to define the deviatoric stress and strain rate tensors,

$$s_{ij} = \sigma_{ij} - \frac{1}{3}\sigma_{kk}\delta_{ij}; \quad \dot{e}_{ij} = \dot{\varepsilon}_{ij} - \frac{1}{3}\dot{\varepsilon}_{kk}\delta_{ij}. \tag{9}$$

We assume, nontrivially, that the total strain rate is the direct sum of elastic, diffusive (corresponding to point defects), and plastic (corresponding to dislocations) contributions,

$$\dot{\varepsilon}_{ij} = \dot{\varepsilon}^{\mathrm{el}}_{ij} + \dot{\varepsilon}^{\mathrm{dif}}_{ij} + \dot{\varepsilon}^{\mathrm{pl}}_{ij}. \tag{10}$$

Then, because dislocation motion is volume-conserving, $\partial U_C/\partial t = s_{ij}\dot{e}^{\mathrm{el}}_{ij}$ (i.e., configurational energy change at constant defect density is simply the deviatoric part of the elastic work—this includes what some authors term "anelasticity," or the reversible rearrangement of defects, that is not plastic in character). As such, Eq. (8) can be recast as

$$\theta\dot{S}_K + \chi\dot{S}_C + \sum_\alpha \left(\frac{\partial U_K}{\partial \eta^\alpha}\right)_{S_K}\dot{\eta}^\alpha + \sum_\beta \left(\frac{\partial U_C}{\partial \rho^\beta}\right)_{S_C}\dot{\rho}^\beta = \sigma_{ij}\left(\dot{\varepsilon}^{\mathrm{dif}}_{ij} + \dot{\varepsilon}^{\mathrm{pl}}_{ij}\right) - \nabla\cdot\mathbf{q}_K - \nabla\cdot\mathbf{q}_C - A(\theta-\theta_0). \tag{11}$$

Meanwhile, the second law of thermodynamics specifies that the entropy production rate per unit volume must be non-negative. Thus,

$$\dot{S}_K + \dot{S}_C + \nabla\cdot\frac{\mathbf{q}_K}{\theta} + \nabla\cdot\frac{\mathbf{q}_C}{\chi} + \frac{A}{\theta}(\theta-\theta_0) + \sum_\alpha \frac{\mu^\alpha f^\alpha}{\Omega_0\theta} - \frac{1}{\Omega_0\theta}\sum_\alpha \nabla\cdot(\mu^\alpha \mathbf{j}^\alpha) \geq 0, \tag{12}$$

where μ^α is the chemical potential of each point defect of species α. To proceed, we multiply Eq. (12) by χ and use Eq. (11) to eliminate $\chi\dot{S}_C$—this is done because the evolution of the configurational subsystem is slower than the kinetic-vibrational subsystem—and use the continuity equation, Eq. (3), alongside Fourier's law for heat conduction. The result is

$$\sigma_{ij}\left(\dot{\varepsilon}^{\mathrm{dif}}_{ij} + \dot{\varepsilon}^{\mathrm{pl}}_{ij}\right) + (\chi-\theta)\left[\dot{S}_K + \frac{A}{\theta}(\theta-\theta_0) - \frac{K_K}{\theta}\nabla^2\theta + \sum_\alpha \frac{\mu^\alpha\dot{\eta}^\alpha}{\Omega_0\theta}\right] + K_K\frac{\chi}{\theta^2}(\nabla\theta)^2 + K_C(\nabla\chi)^2 - \frac{1}{\Omega_0\theta}\sum_\alpha \mathbf{j}^\alpha\cdot\nabla\mu^\alpha - \sum_\alpha\left[\left(\frac{\partial U_K}{\partial\eta^\alpha}\right)_{S_K} - \frac{\mu^\alpha}{\Omega_0}\right]\dot{\eta}^\alpha - \sum_\beta\left(\frac{\partial U_C}{\partial\rho^\beta}\right)_{S_K}\dot{\rho}^\beta \geq 0. \tag{13}$$

Observe that we have separated the left-hand side into independently variable terms and, in particular, one proportional to the temperature difference $\chi-\theta$ between the configurational and kinetic-vibrational subsystems to describe the weak coupling between them. To apply the Coleman–Noll procedure—that is, taking advantage of the fact that each independently variable term must be non-negative to derive thermodynamic constraints and steady-state relationships—we must now supplement the formulation with the appropriate kinematic equations and quantify the contributions of the defects to the energies and entropies. This is done in Secs. III–VIII.

III. VACANCIES AND INTERSTITIALS: KINEMATICS, ENERGY, AND ENTROPY

The creation and diffusional flow of point defects contributes a diffusional strain rate given by

$$\dot{\varepsilon}^{\mathrm{dif}}_{ij} = \sum_\alpha \frac{\gamma^\alpha}{2}\left(\partial_i j^\alpha_j + \partial_j j^\alpha_i\right) + \sum_\alpha \lambda^\alpha\dot{\eta}^\alpha\delta_{ij}, \tag{14}$$

with corresponding deviatoric components

$$\dot{e}_{ij}^{\mathrm{dif}} = \sum_{\alpha} \frac{\gamma^{\alpha}}{2}\left(\partial_i j_j^{\alpha} + \partial_j j_i^{\alpha}\right) - \sum_{\alpha} \frac{\gamma^{\alpha}}{3}\delta_{ij}\partial_k j_k. \tag{15}$$

In Eq. (14), the first term describes the strain rate that results from the velocity gradients of point defects and follows from Ref. 18, with $\gamma^I = 1$ and $\gamma^V = -1$. The second term corresponds to the isotropic strain field generated by point defects, with λ^{α}, $\alpha = I, V$ being dimensionless constants related to the elastic polarizability. Note that the expression in Eq. (14) for the diffusional strain rate differs from that in Ref. 19 by an isotropic term identical to the second term in Eq. (15). The authors in Ref. 19 posited that the extra term would be necessary to separate deviatoric and hydrostatic parts and that hydrostatic parts can be attributed to the strain field of point defects alone. Such a treatment would essentially neglect the hydrostatic part of point-defect flow and is likely incorrect.

Vacancies and interstitials contribute energy through their formation energies e^{α} as well as their interaction with the elastic strain field. The formation energy contribution is given by[12]

$$U^{\mathrm{el}} = -\sum_{\alpha} \eta^{\alpha} P^{\alpha} \varepsilon_{kk}^{\mathrm{el}}, \tag{16}$$

where P^{α}, $\alpha = I, V$ are the isotropic elastic polarizabilities. This can be converted into the form

$$U^{\mathrm{el}} = -\sum_{\alpha} \eta^{\alpha} \lambda^{\alpha} \sigma_{kk}^{\mathrm{el}}, \tag{17}$$

where $\lambda^{\alpha} = P^{\alpha}/(3K)$ is the same λ^{α} that appears in Eq. (14) for the diffusional strain rate, and K is the bulk modulus. (Note that $\lambda^I > 0$ and $\lambda^V < 0$.[12]) Thus, we write for the energy density

$$U_K = U_K^0(\eta^{\alpha}) + U_K^1(S_K^1), \tag{18}$$

where

$$U_K^0(\eta^{\alpha}) = \sum_{\alpha}\left(\frac{e^{\alpha}}{\Omega_0} - \sigma_{kk}\lambda^{\alpha}\right)\eta^{\alpha}, \tag{19}$$

and $U_K^1(S_K^1)$ is the contribution of the thermal energy not associated with point defects. Likewise, for the entropy density,

$$S_K = S_K^0(\eta^{\alpha}) + S_K^1(U_K^1), \tag{20}$$

where

$$S_K^0(\eta^{\alpha}) = -\frac{1}{\Omega_0}\sum_{\alpha}[\eta^{\alpha}\ln\eta^{\alpha} + (1-\eta^{\alpha})\ln(1-\eta^{\alpha})], \tag{21}$$

and S_K^1 is the thermal entropy density not associated with point defects, such that $\theta = \partial U_K^1/\partial S_K^1$.

Returning to the second-law inequality, Eq. (13), the terms related to the motion of point defects are

$$\sigma_{ij}\dot{\varepsilon}_{ij}^{\mathrm{dif}} - \sum_{\alpha}\left(\frac{\partial U_K}{\partial \eta^{\alpha}}\right)_{S_K}\dot{\eta}^{\alpha} + \sum_{\alpha}\frac{\mu^{\alpha}}{\Omega_0}\dot{\eta}^{\alpha} - \frac{1}{\Omega_0\theta}\sum_{\alpha}\mathbf{j}^{\alpha}\cdot\nabla\mu^{\alpha} \geq 0. \tag{22}$$

Noting that

$$\left(\frac{\partial U_K}{\partial \eta^{\alpha}}\right)_{S_K} = \frac{\partial U_K^0}{\partial \eta^{\alpha}} - \theta\frac{\partial S_K^0}{\partial \eta^{\alpha}} = \frac{1}{\Omega_0}\left[e^{\alpha} - \sigma_{kk}\lambda^{\alpha}\Omega_0 + \theta\ln\left(\frac{\eta^{\alpha}}{1-\eta^{\alpha}}\right)\right]; \quad \alpha = I, V, \tag{23}$$

and using Eq. (14) for the diffusional strain rate, the result is

$$\sum_{\alpha}\sigma_{ij}\frac{\gamma^{\alpha}}{2}\left(\partial_i j_j^{\alpha} + \partial_j j_i^{\alpha}\right) - \frac{1}{\Omega_0}\sum_{\alpha}\left[e^{\alpha} + e_b^{\alpha} + \theta\ln\left(\frac{\eta^{\alpha}}{1-\eta^{\alpha}}\right) - \mu^{\alpha}\right]\dot{\eta}^{\alpha} - \frac{1}{\Omega_0\theta}\sum_{\alpha}\mathbf{j}^{\alpha}\cdot\nabla\mu^{\alpha} \geq 0, \tag{24}$$

where $e_b^{\alpha} \equiv -2\sigma_{kk}\lambda^{\alpha}\Omega_0$ is the bulk interaction energy that modulates the diffusion of point defects. Each of the three terms in Eq. (24) must be separately non-negative. The non-negativity constraint on the first term will be imposed separately as part of the flow rule. Meanwhile, non-negativity of the second term holds for arbitrary $\dot{\eta}^{\alpha}$ given by the continuity equation, Eq. (3). As such, the chemical potential must be equal to

$$\mu^{\alpha} = e^{\alpha} + e_b^{\alpha} + \theta\ln\left(\frac{\eta^{\alpha}}{1-\eta^{\alpha}}\right); \quad \alpha = I, V. \tag{25}$$

In particular, at thermal equilibrium $\mu^{\alpha} = 0$, so that the equilibrium fractions of interstitials and vacancies are

$$\eta^{\alpha,\mathrm{eq}} = \left[1 + \exp\left(\frac{e^{\alpha} + e_b^{\alpha}}{\theta}\right)\right]^{-1} \simeq \exp\left(-\frac{e^{\alpha} + e_b^{\alpha}}{\theta}\right); \quad \alpha = I, V. \tag{26}$$

The non-negativity constraint on the third term indicates that the flux of interstitials and vacancies are simply proportional to the negative gradient of their respective chemical potentials; in fact,

$$\mathbf{j}^{\alpha} = -\frac{D_{\alpha}\eta^{\alpha}}{\theta}\nabla\mu^{\alpha}; \quad \alpha = I, V, \tag{27}$$

where D_{α} is the temperature-dependent diffusion coefficient.

IV. DISLOCATION PLASTICITY

Within our isotropic assumption of randomly oriented grains, we can write the plastic strain rate tensor as

$$\dot{\varepsilon}_{ij}^{\mathrm{pl}} = \frac{1}{2}\frac{s_{ij}}{\bar{s}}\dot{\varepsilon}^{\mathrm{pl}}, \tag{28}$$

where, according to Orowan's law,

$$\dot{\varepsilon}^{\mathrm{pl}} = \rho_D b v, \tag{29}$$

where v is the average speed of dislocation motion and, as before, ρ_D is the dislocation line length per unit volume, and b is the length of the Burgers vector. The stress invariant is $\bar{s} = \sqrt{\frac{1}{2} s_{ij} s_{ij}}$. Again, the dimensionless dislocation density is $\rho = a^2 \rho_D$, where $a \sim 10b$. For our purposes, there is no need to resolve the slip systems, and a single, scalar dislocation density would suffice.

The average speed of dislocation motion, v, contains interesting physics. It is equal to the average spacing between dislocations, $l = 1/\sqrt{\rho_D}$, divided by the pinning time τ. (As in Refs. 20 and 21, we do not make the artificial distinction between mobile and immobile dislocations. In face-centered cubic materials such as copper and aluminum, the majority of the dislocations can participate in the glide process, and the density of geometrically necessary dislocations is generally insignificant in the specimen geometry of creep tests.) Dislocations bypass obstacles by means of both diffusion-assisted climb and thermally activated glide, with waiting times τ^{cl} and τ^{gl}, respectively. Thus,

$$\frac{1}{\tau} = \frac{1}{\tau^{\mathrm{cl}}} + \frac{1}{\tau^{\mathrm{gl}}}. \tag{30}$$

As such, the plastic strain rate can be separated into climb and glide contributions,

$$\dot{\varepsilon}^{\mathrm{pl}} = \dot{\varepsilon}^{\mathrm{cl}} + \dot{\varepsilon}^{\mathrm{gl}}. \tag{31}$$

We now evaluate these two contributions separately.

A. Dislocation glide

The dislocation glide contribution to the plastic strain rate, alongside the evolution of the dislocation density, is given by the thermodynamic dislocation theory (TDT),[20–23] which we briefly repeat here. Because dislocation glide is a stress-dependent thermally activated process, the depinning time τ^{gl} appearing in Eq. (30) is given by

$$\frac{1}{\tau^{\mathrm{gl}}} = \frac{1}{\tau_m} \exp\left(-\frac{k_B T_P}{\theta} e^{-\bar{s}/(\alpha_T G \sqrt{\rho})} \right). \tag{32}$$

Here, $\tau_m \sim 10^{-13}$ s is a microscopic time scale, $\theta = k_B T$ is the temperature, and $\bar{s} = \sqrt{\frac{1}{2} s_{ij} s_{ij}}$ is the deviatoric stress invariant. This equation expresses the idea that dislocation depinning is a thermally activated, stress-controlled process that underlies dislocation glide, and that the jumping time of a dislocation line between successive pinning sites is short compared to the wait time at each pinning site. The quantity $k_B T_P$, with T_P in units of Kelvin, measures the energy barrier of dislocation depinning. The proportionality factor for the Taylor stress $\alpha_T \sim \mathcal{O}(0.01)$ measures the slip resistance between a pair of opposing dislocations. The quantity $k_B T_P$, with T_P in units of Kelvin, measures the energy barrier of dislocation depinning. Inserting this back into the Orowan relation, Eq. (29), the glide component of the plastic strain rate is

$$\dot{\varepsilon}^{\mathrm{gl}} = \frac{\sqrt{\rho}}{\tau_0} \exp\left(-\frac{k_B T_P}{\theta} e^{-\bar{s}/(\alpha_T G \sqrt{\rho})} \right), \tag{33}$$

where $\tau_0 = (a/b)\tau_m \simeq 10\tau_m$.

B. Dislocation climb and interaction with point defects

In this subsection, we focus on the climb component, which is associated with the absorption and emission of point defects at dislocations and, as such, contributes to the source term f^{α} in Eq. (3), which we specify below.

The waiting time for dislocation climb is given in terms of the average climb distance $l^{\mathrm{cl}} \simeq 50b \simeq 5a$ and the fraction $f_e \simeq 0.1$ of dislocations that are of edge character as[26–28]

$$\frac{1}{\tau^{\mathrm{cl}}} = \frac{f_e v^{\mathrm{cl}}}{l^{\mathrm{cl}}}. \tag{34}$$

The climb velocity is proportional to the net flux of point defects due to the imbalance between their concentrations near the dislocation core and the bulk of the material,

$$v^{\mathrm{cl}} = \frac{1}{b} \Big[Z_I D_I \big(1 + g^I(\bar{s}, \theta)\big) \big(\eta^I - \eta^{I,\mathrm{core}}\big) - Z_V D_V \big(1 + g^V(\bar{s}, \theta)\big) \big(\eta^V - \eta^{V,\mathrm{core}}\big) \Big], \tag{35}$$

where Z_I and Z_V are the interstitial and vacancy capture efficiencies. This expression differs from the conventional one (see, e.g., Ref. 19) by two correction terms $g^I(\bar{s}, \theta)$ and $g^V(\bar{s}, \theta)$, assumed to be functions of the deviatoric stress invariant $\bar{s} = \sqrt{\frac{1}{2} s_{ij} s_{ij}}$ and the temperature $\theta = k_B T$. As we shall see shortly, under the isotropic assumption—without accounting for slip systems—the correction terms are necessary to account for the nonzero steady-state irradiation creep rate. (Ref. 13 suggests, within the conventional SIPA framework, a correction term proportional to $\bar{s}/\theta$, which indicates an irradiation creep rate that decreases with increasing temperature, and increases linearly with the stress, a result that is not consistent with experiments as discussed later.) Anticipating the temperature and stress dependencies of the steady-state creep rate in Ref. 25, we prescribe that

$$g^I(\bar{s}, \theta) = A_0 \exp\left(-\frac{k_B T_A}{\theta} e^{-\bar{s}/(\kappa^I G)} \right), \quad g^V(\bar{s}, \theta) = A_0 \exp\left(-\frac{k_B T_A}{\theta} e^{-\bar{s}/(\kappa^V G)} \right), \tag{36}$$

where A_0 is a dimensionless constant, G is the temperature-dependent shear modulus, T_A is the activation temperature, and κ^{β}, $\beta = I, V$, are dimensionless proportionality constants. The idea is that elastic interactions between the matrix and the point defects induces a correction to the internal strain and the corresponding climb velocity. Strictly speaking, the bulk modulus and not the shear modulus G is the stress scale relevant to dislocation climb,

but assuming that the Poisson ratio remains constant as a function of temperature, stress, and irradiation dose, we use G instead to eliminate the need for yet another model parameter.

Equation (36) expresses the idea that the dislocation climb velocity is controlled by temperature and stress barriers. In any case, a very nonlinear dependence on the temperature θ and stress $\bar{s}$ is necessary to fit the creep strain. While other forms for $g^I(\bar{s}, \theta)$ and $g^V(\bar{s}, \theta)$ are possible, we shall not investigate such possibilities in the present work.

The equilibrium concentrations of interstitials and vacancies at the dislocation core are modified from the equilibrium concentrations in the crystal bulk [Eq. (26)[by the stress,[13]

$$\eta^{\alpha,\mathrm{core}} = \eta^{\alpha,\mathrm{eq}} \exp\left(-\frac{\gamma^\alpha \Omega_0 \sigma_{kk}}{3\theta}\right) \simeq \exp\left(-\frac{e^\alpha + e_b^\alpha + \gamma^\alpha \Omega_0 \sigma_{kk}/3}{\theta}\right); \quad \alpha = I, V. \tag{37}$$

Combining Eqs. (29), (34), and (35), the result for the climb component of the plastic strain rate is

$$\dot{\varepsilon}^{\mathrm{cl}} = \frac{r_e\sqrt{\rho}}{a^2}\left\{Z_I D_I\left[1 + g^I(\bar{s}, \theta)\right]\left(\eta^I - \eta^{I,\mathrm{core}}\right) - Z_V D_V\left[1 + g^V(\bar{s}, \theta)\right]\left(\eta^V - \eta^{V,\mathrm{core}}\right)\right\}. \tag{38}$$

Here, we defined the parameter $r_e = f_e a/l^{\mathrm{cl}} \simeq 1/50$. To convert this into tensor form, simply multiply by $s_{ij}/(2\bar{s})$.

The source terms for vacancies and interstitials, f^α for $\alpha = I, V$ in Eq. (3), are[29]

$$f^\alpha = p_0 K_0 + \frac{\rho D_\alpha}{a^2} Z_\alpha (\eta^{\alpha,\mathrm{core}} - \eta^\alpha); \quad \alpha = I, V. \tag{39}$$

Here, K_0 is the irradiation damage rate as measured in dpa/s, and $p_0 \simeq 0.3$ is the defect creation efficiency observed in molecular dynamics simulations of displacement cascades.[30,31] We neglect the recombination and self-clustering interactions in this formulation.

Observe that Eq. (39) can be used to derive the steady-state irradiation creep rate attributed to dislocation climb. To see this, set $\dot{\eta}^\alpha = 0$, $\alpha = I, V$, in the continuity equation, Eq. (3), and ignore spatial variations in the point-defect densities and fluxes. Then, with $f^\alpha = 0$ in Eq. (39), direct substitution into Eq. (38) for the creep rate leads to

$$\dot{\varepsilon}^{\mathrm{cl,ss}} = \frac{p_0 K_0 r_e}{\sqrt{\rho}}\left[g^I(\bar{s}, \theta) - g^V(\bar{s}, \theta)\right], \tag{40}$$

where $g^\alpha(\bar{s}, \theta)$, $\alpha = I, V$, are given by Eq. (36). Thus,

$$\dot{\varepsilon}^{\mathrm{cl,ss}} = \frac{p_0 K_0 A_0 r_e}{\sqrt{\rho}}\left[\exp\left(-\frac{k_B T_A}{\theta} e^{-\bar{s}/(\kappa^I G)}\right) - \exp\left(-\frac{k_B T_A}{\theta} e^{-\bar{s}/(\kappa^V G)}\right)\right]. \tag{41}$$

As such, the experimentally measured steady-state creep rate can be used to infer parameters appearing in this equation and, in turn, confirm that such parameter values are reasonable. In particular, in the limit of zero irradiation, $K_0 = 0$, and the corresponding steady-state creep rate associated with dislocation climb equals zero.

C. Energy and entropy of dislocations, and dislocation density evolution

To compute the dislocation contribution to the configurational energy and entropy densities U_C and S_C, the lattice gas approximation is used where imaginary lattice sites are spaced a distance $a \simeq 10b$ apart, the minimum separation between dislocations. Let e^D be the formation energy of a dislocation line at one of these sites. Then, following a procedure similar to that described above for point defects,

$$U_C = U_C^0(\rho) + U_C^1(S_C^1); \quad S_C = S_C^0(\rho) + S_C^1(U_C^1), \tag{42}$$

where superscript 1 refers to residual contributions unrelated to dislocations, and

$$U_C^0(\rho) = \frac{e^D \rho}{a^3}; \quad S_C^0(\rho) = \frac{1}{a^3}(-\rho \ln \rho + \rho). \tag{43}$$

The parts of the second-law inequality, Eq. (13), that are related to dislocation plasticity are

$$\sigma_{ij}\dot{\varepsilon}_{ij}^{\mathrm{pl}} - \left(\frac{\partial U_C}{\partial \rho}\right)_{S_C}\dot{\rho} \geq 0. \tag{44}$$

With the plastic strain rate being proportional to $s_{ij}/\bar{s}$ [see Eqs. (33) and (38)], the contraction with the first term produces a term that is proportional to $s_{ij}s_{ij}/\bar{s} \propto \bar{s}$ and is generically non-negative. Thus, we restrict ourselves to the second term. Note that

$$\left(\frac{\partial U_C}{\partial \rho}\right)_{S_C} = \frac{\partial U_C^0}{\partial \rho} - \chi\frac{\partial S_C^0}{\partial \rho} = \frac{1}{a^3}[e_D + \chi \ln \rho], \tag{45}$$

where, as one may recall, $\chi = \partial U_C/\partial S_C$ denotes the effective temperature. Thus, one can show that the (nonequilibrium) steady-state dislocation density is given by

$$\rho^{\mathrm{ss}} = e^{-e_D/\chi}. \tag{46}$$

In order for the second-law inequality to hold at all times, we propose a dislocation density evolution equation of the form

$$\dot{\rho} = \frac{K_\rho}{\alpha_T G \bar{v}^2} s_{ij}\dot{\varepsilon}_{ij}^{\mathrm{pl}}\left(1 - \frac{\rho}{\rho^{\mathrm{ss}}}\right), \tag{47}$$

where K_ρ is a dimensionless constant, and

$$\bar{v} = \ln\left(\frac{k_B T_P}{\theta}\right) - \ln\left[\ln\left(\frac{\sqrt{\rho}}{q}\right)\right], \tag{48}$$

where

$$q = 2\tau\sqrt{\frac{1}{2}\dot{\varepsilon}_{ij}^{\mathrm{gl}}\dot{\varepsilon}_{ij}^{\mathrm{gl}}} = \sqrt{\rho}\exp\left(-\frac{k_B T_P}{\theta} e^{-\bar{s}/(\alpha_T G\sqrt{\rho})}\right) \tag{49}$$

denotes the dimensionless strain rate for dislocation glide, is inserted to produce the correct strain-hardening behavior.[20]

Note that Eq. (47) for the dislocation density evolution marks a significant departure from conventional treatments in polycrystal plasticity such as Refs. 32–34. Conventional models often assume that $\dot{\rho}$ is proportional to the strain rate. Because the macroscopic strain rate is, strictly speaking, a tensor quantity, this immediately results in a mathematical singularity in the limit of zero strain rate, alongside problems with symmetry as one reverses the strain rate, as is evident in the case of simple shear. Our proposed equation as written, in contrast, suggests that $\dot{\rho}$ is directly proportional to the plastic work rate $s_{ij}\dot{\varepsilon}^{\rm pl}_{ij}$, which itself is a scalar quantity invariant under coordinate transformations, thereby circumventing these issues. Moreover, unlike conventional models, there is no need to attribute the evolution of the dislocation density ρ explicitly to the separate mechanisms of dislocation storage and annihilation. Instead, the term proportional to $1-\rho/\rho^{\rm ss}$ in Eq. (47) simply expresses the idea that ρ evolves to the thermodynamically determined steady-state density $\rho^{\rm ss}$.

Finally, the effective temperature χ increases as a result of plastic work and irradiation damage, as both have the effect of increasing configurational disorder. It has a limiting value of $\chi^{\rm ss} \simeq 0.25\, e_D$, which corresponds to a saturating dislocation density,[20]

$$\dot{\chi} = \left(\frac{K_\chi}{\alpha_T G} s_{ij}\dot{\varepsilon}^{\rm pl}_{ij} + c_\chi K_0\right)\left(1-\frac{\chi}{\chi^{\rm ss}}\right). \tag{50}$$

Here, K_χ is a dimensionless constant and c_χ has the unit of dpa^{-1}. One may ask why we did not include a corresponding K_0-dependent term in Eq. (47) for the dislocation density evolution by irradiation damage. Our reasoning is that for relatively low irradiation dose around 0.01 dpa, similar to that of the experiments we reference below,[25] there is no clear evidence for a significant change in the dislocation line and loop densities.[35–40] It suffices to describe the conversion of small dislocation loops into a network of dislocation lines indirectly via the effective temperature χ. The quantity c_χ may be a function of the temperature, but we do not have sufficient information from Ref. 25 to determine such temperature dependence; thus, we assume that c_χ is a material-dependent constant.

V. SUMMARY: EVOLUTION EQUATIONS

We now summarize the evolution equations that we need to solve for the creep behavior alongside the temporal evolution of point defect and dislocation densities. These are

$$\dot{\sigma}_{ij} = 2G\left(\dot{\varepsilon}_{ij} - \dot{\varepsilon}^{\rm dif}_{ij} - \dot{\varepsilon}^{\rm pl}_{ij}\right) + \lambda\left(\dot{\varepsilon}_{kk} - \dot{\varepsilon}^{\rm dif}_{kk} - \dot{\varepsilon}^{\rm pl}_{kk}\right)\delta_{ij}, \tag{51}$$

$$\dot{\varepsilon}^{\rm pl}_{ij} = \dot{\varepsilon}^{\rm cl}_{ij} + \dot{\varepsilon}^{\rm gl}_{ij}, \tag{52}$$

$$\dot{\varepsilon}^{\rm dif}_{ij} = \sum_\alpha \frac{\gamma^\alpha}{2}\left(\partial_i j^\alpha_j + \partial_j j^\alpha_i\right) + \sum_\alpha \lambda^\alpha \dot{\eta}^\alpha \delta_{ij}, \tag{53}$$

$$\dot{\varepsilon}^{\rm cl}_{ij} = \frac{1}{2}\frac{s_{ij}}{\bar{s}}\frac{r_e\sqrt{\rho}}{a^2}\Big\{Z_I D_I\left[1+g^I(\bar{s},\theta)\right]\left(\eta^I-\eta^{I,\rm core}\right). - Z_V D_V\left[1+g^V(\bar{s},\theta)\right]\left(\eta^V-\eta^{V,\rm core}\right)\Big\}, \tag{54}$$

$$\dot{\eta}^\alpha = -\nabla\cdot \mathbf{j}^\alpha + f^\alpha, \tag{55}$$

$$\mathbf{j}^\alpha = -\frac{D_\alpha \eta^\alpha}{\theta}\nabla\mu^\alpha, \tag{56}$$

$$f^\alpha = p_0 K_0 + \frac{\rho D_\alpha}{a^2} Z_\alpha\left(\eta^{\alpha,\rm core} - \eta^\alpha\right), \tag{57}$$

$$\dot{\rho} = \frac{K_\rho}{\alpha_T G v^2} s_{ij}\dot{\varepsilon}^{\rm pl}_{ij}\left(1-\frac{\rho}{\rho^{\rm ss}}\right), \tag{58}$$

$$\dot{\chi} = \left(\frac{K_\chi}{\alpha_T G} s_{ij}\dot{\varepsilon}^{\rm pl}_{ij} + c_\chi K_0\right)\left(1-\frac{\chi}{\chi^{\rm ss}}\right), \tag{59}$$

with $\alpha = I, V$, and the steady-state defect densities given in Eqs. (26), (37), and (46) above, and $g^I(\bar{s},\theta)$ and $g^V(\bar{s},\theta)$ are given by Eq. (36).

VI. IRRADIATION AND THERMAL CREEP IN COPPER AND ALUMINUM: RESULTS

In this section, we apply the model to the creep behavior in polycrystalline copper and aluminum, as reported by the experiments described in Ref. 25. While there may appear to be many model parameters, only a small fraction of them are calibrated in the present work, since the majority of material parameters are reported elsewhere. For example, parameters that govern the formation and diffusional behavior of point defects are reported in references such as Refs. 41–44, while TDT parameters for copper and aluminum are reported in references such as Refs. 20, 21, and 45. For both copper and aluminum, we assume a temperature-dependent shear modulus of the form

$$G(\theta) = G_0 - \frac{D_0}{e^{k_B T_0/\theta}-1}. \tag{60}$$

We assume that the point-defect diffusion coefficients are temperature-dependent,

$$D_\alpha = D_{\alpha,0} e^{-e^\alpha_m/\theta}, \quad \alpha = I, V, \tag{61}$$

where e^α_m, $\alpha = I, V$, are the migration energies. In addition, because the dislocation formation energy e_D appears only in the combination e_D/χ, we can without loss of generality non-dimensionalize both e_D and the effective temperature χ, and set $e_D = 1$. Values of material parameters used in the present work are listed in Table I, while initial conditions are listed in Table II. In all cases, the initial density of interstitials and vacancies are given by the zero-stress values $\eta^{\alpha,\rm eq}$ at thermal equilibrium, given in

TABLE I. List of parameter values used in the present work. Those with an asterisk (*) are viewed as adjustable and calibrated for the present work.

Symbol	Definition or meaning	Value for Cu	Value for Al	Reference if applicable
G_0	Shear modulus parameter	52 GPa	28.8 GPa	…
D_0	Shear modulus parameter	16.5 GPa	3.44 GPa	…
T_0	Shear modulus parameter	448 K	215 K	…
λ^I	Related to interstitial elastic polarizability	0.67	1	19
λ^V	Related to vacancy elastic polarizability	−0.067	−0.1	19
Z^I	Interstitial capture efficiency	1.0	1.0	19
Z^V	Vacancy capture efficiency	1.2	1.2	19
$D_{I,0}$	Interstitial diffusion coefficient	7.92×10^{-8} m^2 s^{-1}	3.9×10^{-10} m^2 s^{-1}	42 and 44
$D_{V,0}$	Vacancy diffusion coefficient	3.1×10^{-6} m^2 s^{-1}	2.52×10^{-5} m^2 s^{-1}	43 and 44
e_m^I	Interstitial migration energy	0.098 eV	0.1 eV	43 and 44
e_m^V	Vacancy migration energy	0.69 eV	0.73 eV	43 and 44
e^I	Interstitial formation energy	3.07 eV	1.8 eV	42 and 44
e^V	Vacancy formation energy	1.27 eV	0.68 eV	43 and 44
Ω_0	Atomic volume	1.18×10^{-29} m^3	1.66×10^{-29} m^3	…
A_0	Creep rate correction*	1.2×10^5	1.8×10^7	…
T_A	Creep rate correction*	6500 K	2000 K	…
κ^I	Proportionality factor for climb resistance*	1.0×10^{-3}	4.0×10^{-2}	…
κ^V	Proportionality factor for climb resistance*	1.0×10^{-2}	5.0×10^{-2}	…
p_0	Defect creation efficiency	0.3	0.3	29
K_0	Irradiation displacement rate	2×10^{-9} dpa s^{-1}	2×10^{-9} dpa s^{-1}	…
r_e	Scaling parameter	0.02	0.02	27
α_T	Proportionality factor for slip resistance*	0.02	0.04	20 and 45
τ_0	Microscopic time scale	10^{-12} s	10^{-12} s	20 and 21
T_P	Energy barrier to dislocation depinning	40 800 K	24 000 K	20 and 45
e_D	Dislocation formation energy	1	1	…
χ^{ss}	Steady-state effective temperature	0.25	0.25	20 and 21
K_ρ	Hardening rate parameter*	3.1	1.15	45
K_χ	Effective temperature rate coefficient	16.0	3.5	20 and 45
c_χ	Effective temperature rate coefficient*	10 dpa^{-1}	1000 dpa^{-1}	…
a	Microscopic length scale	2.5 nm	2.5 nm	20

Eq. (26). For both samples under irradiation, the fast neutron flux is reported to be 1.4×10^{16} m^{-2} s^{-1}, which translates to a displacement damage rate of $K_0 = 2 \times 10^{-9}$ s^{-1}. As we indicated in Table II, the majority of parameter values are well-accepted or taken from the literature, and only a small handful—those marked with an asterisk—are adjustable for the purpose of this work. We note that the results are apparently not overly sensitive to the majority of adjustable parameters, but very sensitive to the hardening rate parameter K_ρ—which, being dependent on the grain size,[21] is viewed as adjustable—as well as the initial dislocation density $\rho(t = 0)$.

A. Accumulated creep strain

We consider isotropic and homogeneous samples of copper and aluminum held at several values of fixed von Mises stress $\sigma = \sqrt{3}\bar{s}$ and temperature and neglect spatial variation of dislocation configuration as well as interstitial and vacancy concentration; as such, the point-defect currents are identically zero: $j^\alpha = 0$ for $\alpha = I, V$. With a zero elastic strain rate alongside a zero deviatoric diffusion strain rate $\dot{e}_{ij}^{\rm dif}$, we compute the creep strain by integrating the invariant plastic strain rate, which equals the sum of the glide and climb components,

$$\dot{\varepsilon} = \dot{\varepsilon}^{\rm pl} = \dot{\varepsilon}^{\rm gl} + \dot{\varepsilon}^{\rm cl}, \tag{62}$$

over time. The result is shown in Fig. 1. Note that the apparent nonzero creep rate in the irradiated samples justifies the correction terms to the climb velocity in Eq. (35) and the climb component of the strain rate in Eq. (38), and that the steady-state creep rate given by Eq. (40) can be used to aid the determination of fitting parameters.

TABLE II. Initial conditions.

Symbol	Definition or meaning	Value for Cu	Value for Al
ρ	Dislocation density	3×10^{-3}	3.2×10^{-4}
χ	Effective temperature	0.21	0.2

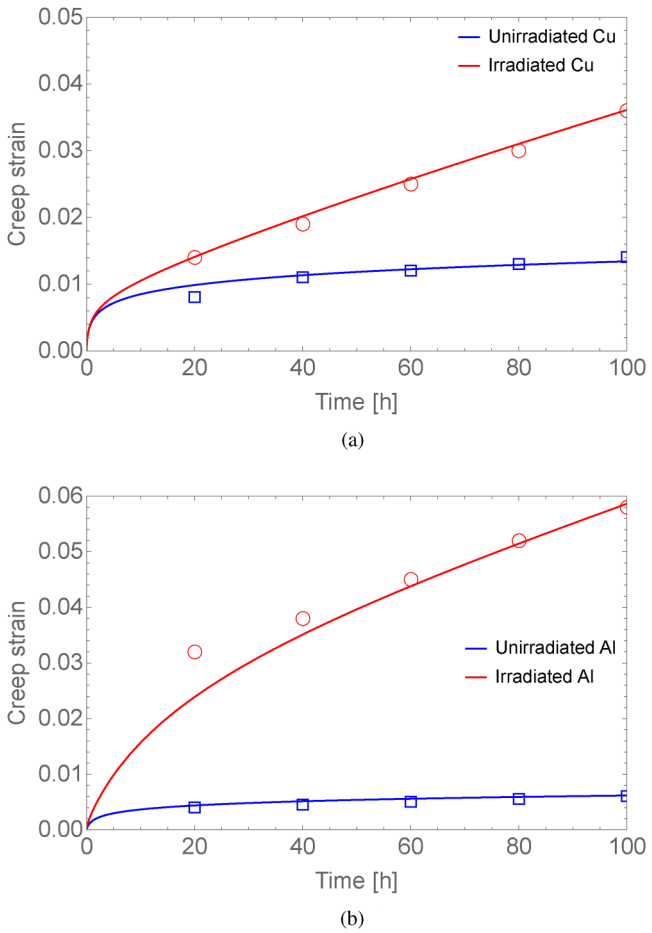

FIG. 1. Creep strain as a function of time for both irradiated and unirradiated (a) copper at $\sigma = 57$ MPa and $T = 523$ K, and (b) aluminum at $\sigma = 14.7$ MPa and $T = 393$ K. The open symbols represent the experimental data from Ref. 25 while the lines represent model results. (a) Cu, $\sigma = 57$ MPa, $T = 523$ K, (b) Al, $\sigma = 14.7$ MPa, $T = 393$ K.

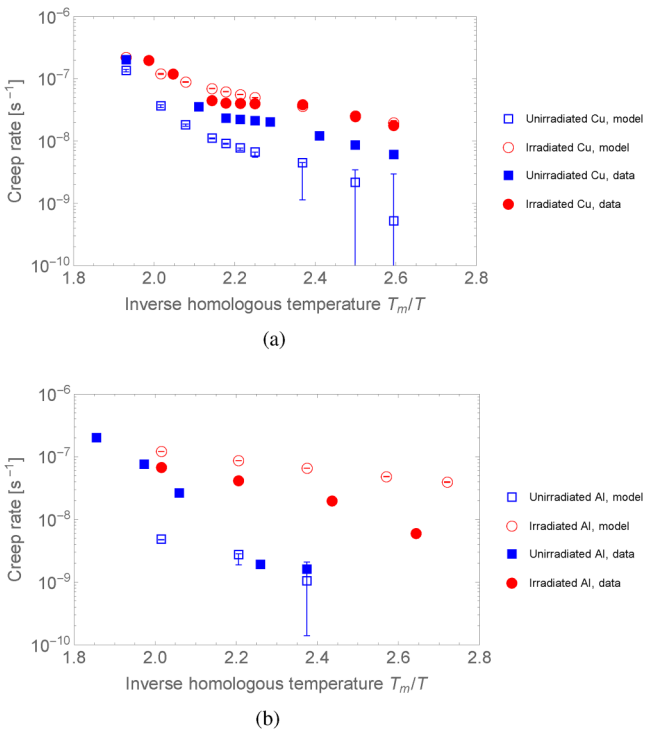

FIG. 2. Steady-state creep rate at several homologous temperatures, computed by evaluating the plastic strain rate $\dot{\varepsilon}^{\mathrm{pl}}$ at time $t = 100$ h, for both irradiated and unirradiated (a) copper at $\sigma = 40$ MPa, and (b) aluminum at $\sigma = 10$ MPa. The error bars indicate uncertainties with the initial dislocation densities, as discussed in the main text. (a) Cu, $\sigma = 40$ MPa, (b) Al, $\sigma = 14.7$ MPa.

B. Dependence of creep rate on temperature

We now discuss the temperature dependence of the steady-state creep rate. Figure 2 shows the steady-state creep rate at several temperatures, computed by evaluating the plastic strain rate $\dot{\varepsilon}^{\mathrm{pl}}$ at time $t = 100$ h, for both irradiated and unirradiated copper and aluminum, held at fixed stress $\sigma = 40$ and 10 MPa, respectively. In fitting the model to the data we primarily used the low-temperature creep rates to determine the parameters in Eq. (40)—notably A_0, T_A, κ^I in the case of copper, and α^V in the case of aluminum—with the knowledge that the irradiation creep rate at long times is at least an order of magnitude higher than the component of the creep rate attributed to dislocation glide alone at low temperatures. As it turns out, this provides very good agreement—and we are able to capture, at least qualitatively, the crossover between low ($T < 0.4T_m$) and high ($T > 0.5T_m$) homologous temperature data for copper, where T_m is the melting temperature. The agreement between the model and data is less good for the unirradiated samples undergoing thermal creep.

We suspect that this discrepancy can be traced to uncertainties in the initial dislocation density. Indeed, in computing the model results in this manuscript, we primarily used the creep strain as a function of time of copper at $T = 523$ K and $\sigma = 57$ MPa, and aluminum at $T = 393$ K and $\sigma = 14.7$ MPa, as shown in Fig. 1, to determine the initial dislocation density and the hardening rate parameter K_ρ. These are the only such curves available in Ref. 25. This results in a discrepancy ranging between a factor of four and ten in the steady-state thermal creep rate in unirradiated copper at lower temperatures and $\sigma = 40$ MPa in Fig. 1(a). We emphasize, however, that the thermal creep rate is extremely low in any case, of the order of 10^{-9} s^{-1}. Moreover, from Eq. (33), the component of the plastic strain rate attributed to dislocation glide is a very nonlinear and sensitive function of the dislocation density as well as the temperature; a variation of the dislocation density by about 10% leads to a factor-of-two difference in the thermal creep rate, and varying the dislocation density by a factor of two can alter the thermal creep rate by one to two orders of magnitude. To illustrate this pronounced nonlinearity, the open symbols in Fig. 2(a) are

supplemented with error bars that indicate the creep rates for initial dislocation densities $\rho = 1.5 \times 10^{-3}$ (upper limit of the error bar) and $\rho = 4.5 \times 10^{-3}$ (lower limit of the error bar), at $\pm 50\%$ the assumed initial dislocation density of $\rho = 3.0 \times 10^{-3}$, or $\rho_D = 4.8 \times 10^{14}\,\mathrm{m}^{-2}$. Meanwhile, the error bars for the model results in Fig. 2(b) indicate the creep rates for dislocation densities ranging between $\rho = 1.6 \times 10^{-4}$ and 4.8×10^{-4}, or $\pm 50\%$ the assumed initial dislocation density of $\rho = 3.2 \times 10^{-4}$, or $\rho_D = 5.12 \times 10^{13}\,\mathrm{m}^{-2}$. Given inherent uncertainties in the initial dislocation density, we suspect that we might be able to attain much better agreement between model and experiment if we adjust the initial dislocation density individually for each temperature sampled, but we made no attempt to do so for clarity.

C. Dependence of creep rate on stress

The variation of the steady-state creep rate with stress is shown in Fig. 3, for copper at temperature $T = 523\,\mathrm{K}$ and aluminum at $T = 353\,\mathrm{K}$. As in the case of Fig. 2 for the variation with temperature at fixed stress, we find much better agreement for the irradiated than for the unirradiated materials in which only thermal creep is present and is dominated by dislocation glide in the long-time limit. Here, we also made no attempt to adjust the initial dislocation density individually for each stress level, instead keeping it fixed at $\rho = 3 \times 10^{-3}$ for copper, with error bars indicating variation between $\rho = 2 \times 10^{-3}$ and 4×10^{-3}; and at $\rho = 3.2 \times 10^{-4}$ for aluminum, with error bars indicating variation between $\rho = 1.6 \times 10^{-4}$ and 4.8×10^{-4}. Note that the very pronounced stress dependence of the irradiation creep rate, almost resembling a power law and illustrated by the red symbols in Fig. 3, in part motivates the very nonlinear correction terms for the climb velocity in Eqs. (35) and (36). A simple linear dependence of the irradiation creep rate on the deviatoric stress s_{ij}, such as in Ref. 13, will not reproduce the stress dependence of the steady-state creep rate.

D. Relative contributions of dislocation glide and climb

We now compute relative contributions of the glide and climb components, $\dot{\varepsilon}^{\mathrm{gl}}$ and $\dot{\varepsilon}^{\mathrm{cl}}$, to the total creep rate $\dot{\varepsilon}^{\mathrm{pl}}$, by computing the ratios $\dot{\varepsilon}^{\mathrm{gl}}/\dot{\varepsilon}^{\mathrm{pl}}$ and $\dot{\varepsilon}^{\mathrm{cl}}/\dot{\varepsilon}^{\mathrm{pl}}$. For concreteness, we restrict ourselves to the stress and temperature conditions corresponding to the creep strains depicted in Fig. 1; the result is shown in Fig. 4. We note that at sufficiently long times, the climb component dominates irradiation creep, while the glide component dominates in the unirradiated cases, for which the vacancy-mediated climb component is vanishingly small. Interestingly, the transition to long-time behavior is much more gradual in copper than in aluminum, in which nearly all of the irradiation creep is attributed to dislocation climb right at the outset.

E. Dislocation density evolution

Figure 5 shows the temporal evolution of the dimensionless dislocation density ρ for both irradiated and unirradiated copper and aluminum under the conditions described in Fig. 1. In both copper and aluminum, the dislocation density grows much more

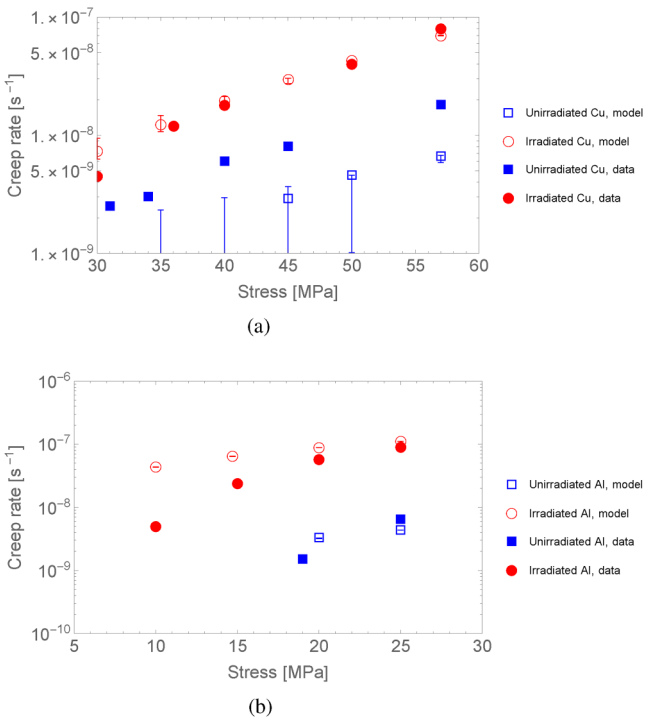

FIG. 3. Steady-state creep rate at several stress values σ, computed by evaluating the plastic strain rate $\dot{\varepsilon}^{\mathrm{pl}}$ at time $t = 100$ h, for both irradiated and unirradiated (a) copper at $T = 523$ K, and (b) aluminum at $T = 353$ K. The error bars indicate uncertainties with the initial dislocation densities, as discussed in the main text. (a) Cu, $T = 523$ K, (b) Al, $T = 353$ K.

substantially under irradiation than without. Tracing this back to the dislocation density evolution equation, Eq. (47), this can be attributed to the elevated creep rate in the irradiated material compared to its unirradiated counterpart. This, in turn, is attributed to dislocation climb mediated by point-defect production and absorption, as described by Eq. (38).

At this point, it is instructive to investigate how the parameter c_χ, first introduced in Eq. (50) to describe the effect of irradiation damage on configurational disorder, influences irradiation creep. To this end, Fig. 6 compares the irradiation creep strain for aluminum given by our model, with $c_\chi = 1000$ as in Fig. 1(b) and elsewhere in this paper, alongside the hypothetical irradiation creep strain computed by setting $c_\chi = 0$ and otherwise identical model parameters. While both values of c_χ give rise to the same steady-state creep rate, the creep enhancement at early times given by setting a nonzero value of c_χ is very much discernible and is needed to fit the experimental data. Our interpretation is that the irradiation-induced increase in configurational disorder is correlated with an increase in the dislocation loop length, and, hence, the dislocation density, through an elevated value of ρ^{ss} in Eq. (47). This may be connected to stress-induced preferential nucleation (SIPN), recently confirmed in experiments and simulations.[46]

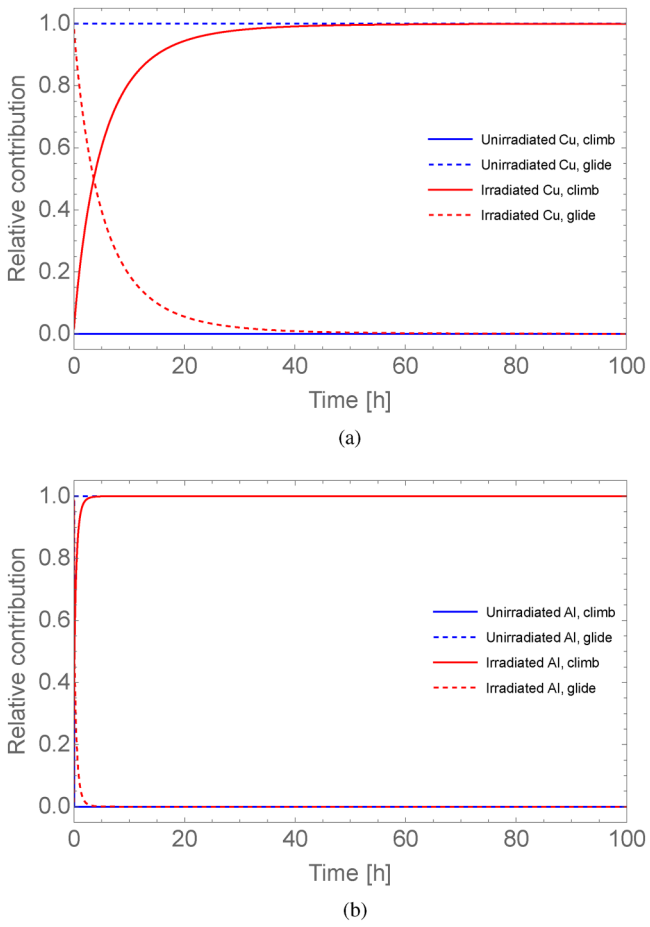

FIG. 4. Relative contributions of the glide and climb components, $\dot{\varepsilon}^{gl}$ and $\dot{\varepsilon}^{cl}$, to the total creep rate $\dot{\varepsilon}^{pl}$, for both irradiated and unirradiated (a) copper at $\sigma = 57$ MPa and $T = 523$ K, and (b) aluminum at $\sigma = 14.7$ MPa and $T = 393$ K. (a) Cu, $\sigma = 57$ MPa, $T = 523$ K, (b) Al, $\sigma = 14.7$ MPa, $T = 393$ K.

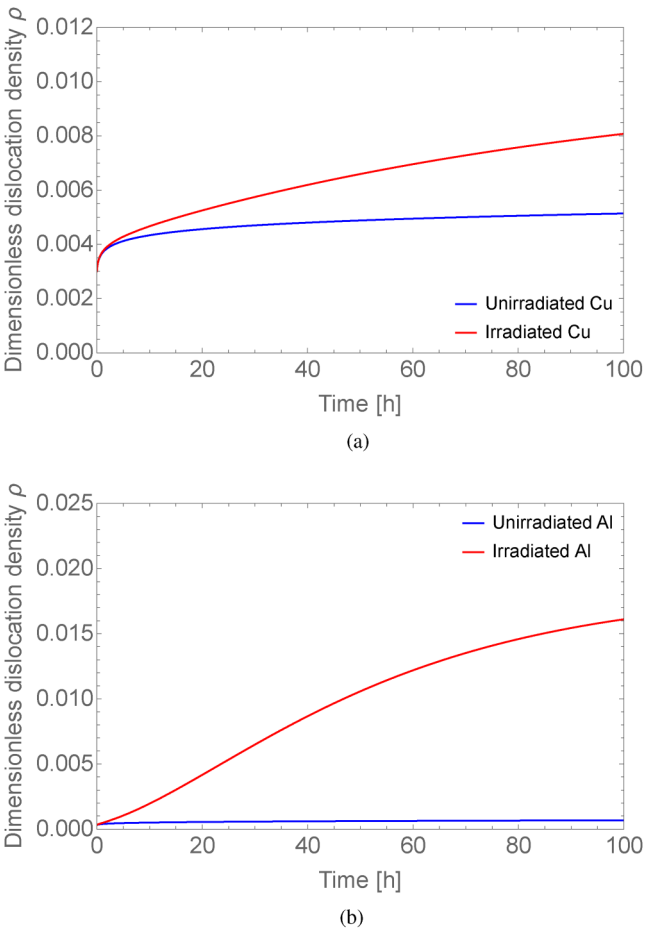

FIG. 5. Evolution of the dimensionless dislocation density ρ for both irradiated and unirradiated (a) copper at $\sigma = 57$ MPa and $T = 523$ K, and (b) aluminum at $\sigma = 14.7$ MPa and $T = 393$ K. To obtain the dislocation density in units of m^{-2}, divide the dimensionless value by $a^2 = 6.25 \times 10^{-18}\,m^{-2}$. (a) Cu, $\sigma = 57$ MPa, $T = 523$ K, (b) Al, $\sigma = 14.7$ MPa, $T = 393$ K.

F. Validity of conventional SIPA mechanism

We are now in a position to determine the parameter regime where the correction terms $g^I(\bar{s}, \theta)$ and $g^V(\bar{s}, \theta)$ introduced in Eq. (35) for the dislocation climb velocity and written out in full in Eq. (36) are significant. From Eqs. (35) and (40), we can heuristically regard conventional SIPA to be a reasonably good approximation if

$$g^I(\bar{s}, \theta) - g^V(\bar{s}, \theta) < 1. \tag{63}$$

The shaded regions in each of the panels in Fig. 7 depict the parameter regime in which conventional SIPA provides a good approximation for irradiation creep in copper and aluminum—namely, at sufficiently low temperatures ($T < 0.1\,T_m$) if the stress exceeds $\sigma = 0.002\,\mu$, or low stresses at higher temperatures.

VII. DISCUSSION

The steady-state irradiation creep rate in conventional SIPA scales linearly with the stress σ and inversely with the temperature $\theta = k_B T$. In-reactor measurements described in Ref. 25 seem to contradict this notion. Indeed, we have shown that temperature- and stress-dependent correction terms $g^I(\bar{s}, \theta)$ and $g^V(\bar{s}, \theta)$ must be added to the conventional SIPA creep rate to describe the power-law-like scaling with the stress. The correction terms can be easily understood as a manifestation of temperature-dependent stress activation of dislocation climb, akin to the thermally activated depinning in dislocation glide.[20] We recover the conventional SIPA creep rate at low temperatures and stresses. We emphasize that in no way are we suggesting that the SIPA mechanism itself is incorrect; rather, our model for point-defect absorption is based on the SIPA framework, and one of our key propositions is that we must

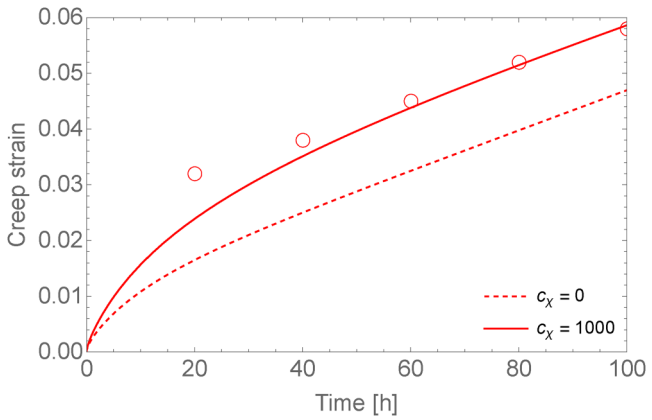

FIG. 6. Comparison of model creep strain in irradiated aluminum at $\sigma = 14.7$ MPa and $T = 393$ K, with $c_\chi = 1000$ (solid curve) and 0 (dashed curve), respectively, to illustrate the effect of the parameter c_χ, which describes the increase in configurational disorder due to irradiation.

modify the SIPA creep rate to describe the set of in-reactor creep measurements that we referenced in our work.

Thus far, we have, for simplicity, assumed spatial homogeneity and neglected the point-defect diffusion terms proportional to $\mathbf{j}^\alpha$, $\alpha = I, V$. For neutron irradiation, the damage rate K_0 is uniform throughout the sample, and at sufficiently long times, the point-defect densities will approach their respective steady-state values given by setting $f^\alpha = 0$ in Eq. (39), becoming spatially uniform. This justifies our simplification, especially if we primarily focus on steady-state irradiation creep. The extent to which point-defect diffusion influences transient creep within the present model will be investigated in future work; this will call for full-field finite element simulations, beyond the scope of the present manuscript.

A distinguishing feature of our model is the attribution of point defects to the kinetic-vibrational degrees of freedom, and extended defects such as dislocations to the configurational degrees of freedom, the latter of which is described by an effective temperature χ that differs from the actual temperature $\theta = k_B T$. Our rendition of nonequilibrium statistical thermodynamics differs from that in the recent series of papers by McDowell,[47–49] who proposes that a single temperature would suffice with the summation of constrained local equilibrium states and the introduction of long-range athermal stresses. The latter approach has great utility and is capable of resolving structural heterogeneities as well as their interactions by, for instance, regarding grains of different orientations as distinct configurational subsystems. In contrast, our approach is valid over somewhat higher length scales, instead coarse-graining over structural heterogeneities and long-range interactions, while still capturing emergent phenomena produced by an evolving population of dislocations through the effective temperature (but see, e.g., Ref. 23 for how grain boundaries can be described within the TDT framework). The effective temperature has been measured in simulations of other deforming systems[50–52] via fluctuation–dissipation relations or direct computation of the interatomic potential

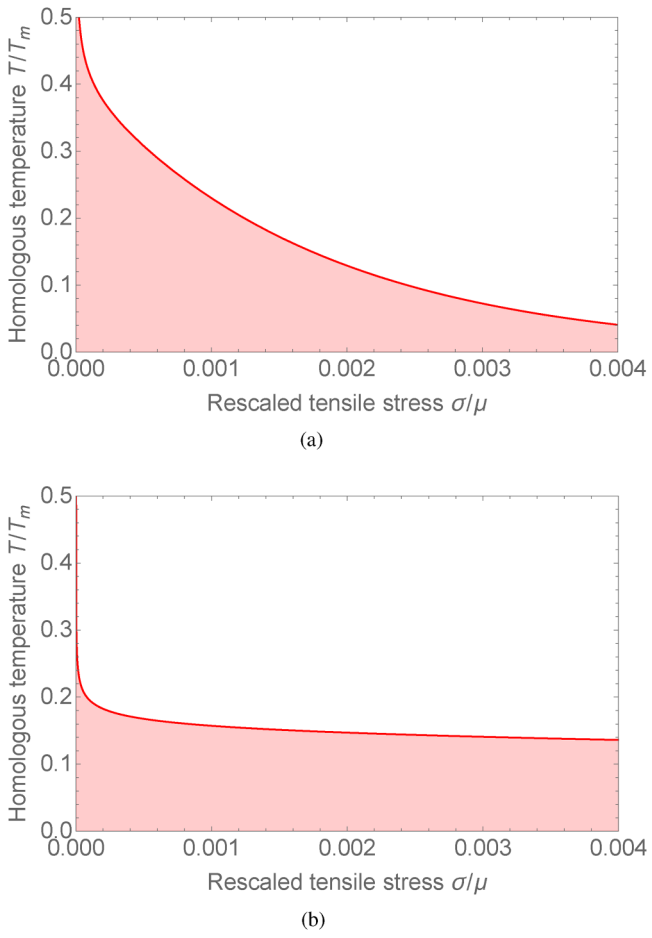

FIG. 7. Plot of the curve $g^I(\bar{s}, \theta) - g^V(\bar{s}, \theta) = 1$ for irradiated (a) copper and (b) aluminum, with both axes non-dimensionalized such that the tensile stress $\sigma = \sqrt{3}\bar{s}$ is measured in units of μ, and the temperature $T = \theta/k_B$ is in units of the melting temperature T_m. In both panels, the shaded region, corresponding to $g^I(\bar{s}, \theta) - g^V(\bar{s}, \theta) < 1$, is the parameter regime in which conventional SIPA is a good approximation of irradiation creep. (a) Cu, (b) Al.

energy. While these references were focused on amorphous systems, we believe the measurement of the effective temperature in MD simulations using similar methods could also assess dislocation-obstacle processes that could inform our model framework and potentially enhance the validity and utility of our proposed approach. If similar measurements can also be done for an irradiated crystalline material, this will help inform model ingredients and significantly enhance the validity and utility of our proposed approach.

The reader may wonder why we did not explicitly model processes such as stress-induced preferential nucleation (SIPN) of dislocation loops,[46] the preferential absorption of suitably oriented loops by dislocations, and loop growth due to stress-induced vacancy emission, in conjunction with SIPA. Our answer is one of

model philosophy. As a starting point, it may be more prudent to only include the most essential processes as model ingredients, so that we do not overcomplicate the physical picture, while still being able to tease out the pertinent aspects of model behavior. The effects of processes we do not explicitly include in the model are likely second-order. However, these processes are still implicitly included in the model. Thus, for example, the nucleation and growth of dislocation loops under irradiation is described by the irradiation-induced increase in configurational disorder [Eq. (50)], which, in turn, facilitates an increased target dislocation density ρ^{ss}, thereby resulting in an increased rate of growth of dislocation line length per unit volume in Eq. (47). This is driven almost entirely by principles of statistical thermodynamics, and our treatment goes on to demonstrate the entropic aspect of processes such as dislocation loop growth.

The irradiation dose in the present study is relatively small—of the order of 0.02 dpa at the end of the calculations. An irradiation dose of 1 dpa or above is known to result in the formation of a high density of defect clusters including cavities and dislocation loops,[35–40] but there appear to be few if any measurements of creep strain in copper and aluminum at such high doses. Important questions to ask in future work include: does our model correctly predict the dislocation microstructure and the irradiation creep strain at high doses? How do cavities influence the *in situ* creep behavior? What model modifications should be made to account for cavities? Would the combination of the present model with cluster dynamics, in a manner akin to Ref. 53 which developed a combined crystal plasticity and cluster dynamics framework, provide a plausible pathway?

VIII. CONCLUSIONS

In this paper, we propose a thermodynamically consistent model for irradiation creep. The model directly references the diffusion of point defects, stress-induced preferential absorption (SIPA) of point defects at dislocations, and the thermodynamic dislocation theory (TDT). Quantification of the contributions of point defects and dislocations to the energy and entropy of the material undergoing creep enables us to deduce the evolution equations for defect densities. *In situ* measurements of in-reactor irradiation creep indicate that a correction to the conventional SIPA dislocation climb rate must be added to account for irradiation creep at high stresses and temperatures. Including such a correction results in a qualitative explanation for the pronounced stress and temperature dependence of the steady-state irradiation creep rate.

ACKNOWLEDGMENTS

The authors acknowledge financial support at the University of Tennessee, Knoxville from the U.S. Department of Energy, Fusion Energy Sciences under Grant No. DE-SC0023180, as well as helpful discussions with Dr. Laurent Capolungo (LANL) and Professor G. Robert Odette (UCSB).

AUTHOR DECLARATIONS

Conflict of Interest

The authors have no conflicts to disclose.

Author Contributions

Charles K. C. Lieou: Conceptualization (equal); Formal analysis (equal); Investigation (equal); Methodology (equal); Visualization (equal); Writing – original draft (equal); Writing – review & editing (equal). **Brian D. Wirth:** Conceptualization (equal); Investigation (equal); Project administration (equal); Resources (equal); Supervision (equal); Writing – review & editing (equal).

DATA AVAILABILITY

The data that support the findings of this study are available from the corresponding author upon reasonable request.

REFERENCES

[1]S. Takeuchi and A. S. Argon, "Steady-state creep of single-phase crystalline matter at high temperature," J. Mater. Sci. **11**, 1542–1566 (1976).
[2]C. Herring, "Diffusional viscosity of a polycrystalline solid," J. Appl. Phys. **21**(5), 437–445 (1950).
[3]F. R. N. Nabarro, "Steady-state diffusional creep," Philos. Mag. **16**(140), 231–237 (1967).
[4]J. Weertman, "Theory of steady-state creep based on dislocation climb," J. Appl. Phys. **26**(10), 1213–1217 (1955).
[5]J. H. Gittus, "Theory of dislocation-creep due to the Frenkel defects or interstitialcies produced by bombardment with energetic particles," Philos. Mag. **25**(2), 345–354 (1972).
[6]R. Sandström, "On recovery of dislocations in subgrains and subgrain coalescence," Acta Metall. **25**(8), 897–904 (1977).
[7]R. Sandstträm, "Subgrain growth occurring by boundary migration," Acta Metall. **25**(8), 905–911 (1977).
[8]B. T. Kelly and A. J. E. Foreman, "The theory of irradiation creep in reactor graphite—The dislocation pinning-unpinning model," Carbon **12**(2), 151–158 (1974).
[9]J. R. Matthews and M. W. Finnis, "Irradiation creep models—An overview," J. Nucl. Mater. **159**, 257–285 (1988).
[10]P. T. Heald and M. V. Speight, "Steady-state irradiation creep," Philos. Mag. **29**(5), 1075–1080 (1974).
[11]R. Bullough and J. R. Willis, "The stress-induced point defect-dislocation interaction and its relevance to irradiation creep," Philos. Mag. **31**(4), 855–861 (1975).
[12]W. G. Wolfer and M. Ashkin, "Stress-induced diffusion of point defects to spherical sinks," J. Appl. Phys. **46**(2), 547–557 (1975).
[13]W. G. Wolfer and M. Ashkin, "Diffusion of vacancies and interstitials to edge dislocations," J. Appl. Phys. **47**(3), 791–800 (1976).
[14]F. Onimus, T. Jourdan, C. Xu, A. A. Campbell, and M. Griffiths, "1.10—Irradiation creep in materials," in *Comprehensive Nuclear Materials*, 2nd ed., edited by R. J. M. Konings and R. E. Stoller (Elsevier, Oxford, 2020), pp. 310–366.
[15]C. McElfresh, Y. Cui, S. L. Dudarev, G. Po, and J. Marian, "Discrete stochastic model of point defect-dislocation interaction for simulating dislocation climb," Int. J. Plast. **136**, 102848 (2021).
[16]C. McElfresh, N. Bertin, S. Aubry, and J. Marian, "Coalescence dynamics of prismatic dislocation loops due to vacancy supersaturation," Phys. Rev. Mater. **6**, L100601 (2022).
[17]V. Berdichevsky, P. Hazzledine, and B. Shoykhet, "Micromechanics of diffusional creep," Int. J. Eng. Sci. **35**(10), 1003–1032 (1997).
[18]A. Villani, E. P. Busso, and S. Forest, "Field theory and diffusion creep predictions in polycrystalline aggregates," Modell. Simul. Mater. Sci. Eng. **23**(5), 055006 (2015).
[19]A. Chakraborty, R. A. Lebensohn, and L. Capolungo, "Coupled chemo-mechanical modeling of point-defect diffusion in a crystal plasticity fast Fourier transform framework," J. Mech. Phys. Solids **173**, 105190 (2023).

[20]J. S. Langer, E. Bouchbinder, and T. Lookman, "Thermodynamic theory of dislocation-mediated plasticity," Acta Mater. **58**(10), 3718–3732 (2010).
[21]J. S. Langer, "Statistical thermodynamics of strain hardening in polycrystalline solids," Phys. Rev. E **92**, 032125 (2015).
[22]C. K. C. Lieou and C. A. Bronkhorst, "Dynamic recrystallization in adiabatic shear banding: Effective-temperature model and comparison to experiments in ultrafine-grained titanium," Int. J. Plast. **111**, 107–121 (2018).
[23]C. K. C. Lieou, H. M. Mourad, and C. A. Bronkhorst, "Strain localization and dynamic recrystallization in polycrystalline metals: Thermodynamic theory and simulation framework," Int. J. Plast. **119**, 171–187 (2019).
[24]C. K. C. Lieou and C. A. Bronkhorst, "Thermomechanical conversion in metals: Dislocation plasticity model evaluation of the Taylor-Quinney coefficient," Acta Mater. **202**, 170–180 (2021).
[25]S. S. Ibragimov, E. S. Aitkhozhin, and Y. S. Pyatiletov, "Radiation-induced creep of aluminum and copper," in *Influence of Radiation on Material Properties: 13th International Symposium (Part II)* (ASTM International, 1987).
[26]A. Patra and D. L. McDowell, "Crystal plasticity-based constitutive modelling of irradiated BCC structures," Philos. Mag. **92**(7), 861–887 (2012).
[27]W. Wen, L. Capolungo, A. Patra, and C. N. Tomé, "A physics-based crystallographic modeling framework for describing the thermal creep behavior of Fe-Cr alloys," Metall. Mater. Trans A **48**, 2603–2617 (2017).
[28]N. Bieberdorf, A. Tallman, M. Arul Kumar, V. Taupin, R. A. Lebensohn, and L. Capolungo, "A mechanistic model for creep lifetime of ferritic steels: Application to Grade 91," Int. J. Plast. **147**, 103086 (2021).
[29]W. Wen, A. Kohnert, M. Arul Kumar, L. Capolungo, and C. N. Tomé, "Mechanism-based modeling of thermal and irradiation creep behavior: An application to ferritic/martensitic HT9 steel," Int. J. Plast. **126**, 102633 (2020).
[30]D. J. Bacon, Y. N. Osetsky, R. Stoller, and R. E. Voskoboinikov, "MD description of damage production in displacement cascades in copper and α-iron," J. Nucl. Mater. **323**(2), 152–162 (2003).
[31]W. Setyawan, A. P. Selby, N. Juslin, R. E. Stoller, B. D. Wirth, and R. J. Kurtz, "Cascade morphology transition in BCC metals," J. Phys.: Cond. Mat. **27**(22), 225402 (2015).
[32]H. Mecking and U. F. Kocks, "Kinetics of flow and strain-hardening," Acta Metall. **29**(11), 1865–1875 (1981).
[33]A. Arsenlis and D. M. Parks, "Modeling the evolution of crystallographic dislocation density in crystal plasticity," J. Mech. Phys. Solids **50**(9), 1979–2009 (2002).
[34]N. R. Barton, A. Arsenlis, and J. Marian, "A polycrystal plasticity model of strain localization in irradiated iron," J. Mech. Phys. Solids **61**(2), 341–351 (2013).
[35]B. N. Singh and S. J. Zinkle, "Defect accumulation in pure FCC metals in the transient regime: A review," J. Nucl. Mater. **206**(2–3), 212–229 (1993).
[36]S. J. Zinkle and K. Farrell, "Void swelling and defect cluster formation in reactor-irradiated copper," J. Nucl. Mater. **168**(3), 262–267 (1989).
[37]S. J. Zinkle, "Radiation-induced effects on microstructure," in *Comprehensive Nuclear Materials*, edited by R. J. M. Konings (Elsevier, Oxford, 2012), pp. 65–98.
[38]S. J. Zinkle, A. Horsewell, B. N. Singh, and W. F. Sommer, "Defect microstructure in copper alloys irradiated with 750 MeV protons," J. Nucl. Mater. **212–215**, 132–138 (1994).
[39]S. J. Zinkle and L. L. Snead, "Microstructure of copper and nickel irradiated with fission neutrons near 230 °C," J. Nucl. Mater. **225**, 123–131 (1995).
[40]S. J. Zinkle and B. N. Singh, "Microstructure of Cu–Ni alloys neutron irradiated at 210 °C and 420 °C to 14 dpa," J. Nucl. Mater. **283-287**, 306–312 (2000).
[41]N. Q. Lam, L. Dagens, and N. V. Doan, "Calculations of the properties of self-interstitials and vacancies in the face-centred cubic metals Cu, Ag and Au," J. Phys. F: Met. Phys. **13**(12), 2503 (1983).
[42]B. J. Jesson, M. Foley, and P. A. Madden, "Thermal properties of the self-interstitial in aluminum: An ab initio molecular-dynamics study," Phys. Rev. B **55**, 4941–4946 (1997).
[43]M. I. Mendelev and B. S. Bokstein, "Molecular dynamics study of vacancy migration in Al," Mater. Lett. **61**(14), 2911–2914 (2007).
[44]A. B. Sivak, D. N. Demidov, and P. A. Sivak, "Diffusion characteristics of self-point defects in copper: Molecular dynamic study," Phys. Atom. Nuclei **85**, 1245–1255 (2022).
[45]K. C. Le, T. M. Tran, and J. S. Langer, "Thermodynamic dislocation theory of high-temperature deformation in aluminum and steel," Phys. Rev. E **96**, 013004 (2017).
[46]D. Da Fonseca, F. Mompiou, T. Jourdan, J.-P. Crocombette, A. Chartier, and F. Onimus, "Evidence of dislocation loop preferential nucleation in irradiated aluminum under stress," Scr. Mater. **233**, 115510 (2023).
[47]D. L. McDowell, "Nonequilibrium statistical thermodynamics of thermally activated dislocation ensembles: Part 1: Subsystem reactions under constrained local equilibrium," J. Mater. Sci. **59**, 5093–5125 (2024).
[48]D. L. McDowell, "Nonequilibrium statistical thermodynamics of thermally activated dislocation ensembles: Part 2—Ensemble evolution toward correlation of enthalpy barriers," J. Mater. Sci. **59**, 5126–5160 (2024).
[49]D. L. McDowell, "Nonequilibrium statistical thermodynamics of thermally activated dislocation ensembles: Part 3—Taylor–Quinney coefficient, size effects and generalized normality," J. Mater. Sci. **59**, 5161–5200 (2024).
[50]C. S. O'Hern, A. J. Liu, and S. R. Nagel, "Effective temperatures in driven systems: Static versus time-dependent relations," Phys. Rev. Lett. **93**, 165702 (2004).
[51]T. K. Haxton and A. J. Liu, "Activated dynamics and effective temperature in a steady state sheared glass," Phys. Rev. Lett. **99**, 195701 (2007).
[52]A. R. Hinkle, C. H. Rycroft, M. D. Shields, and M. L. Falk, "Coarse graining atomistic simulations of plastically deforming amorphous solids," Phys. Rev. E **95**, 053001 (2017).
[53]Q. Yu, G. Po, and J. Marian, "Physics-based model of irradiation creep for ferritic materials under fusion energy operation conditions," J. Appl. Phys. **132**(22), 225101 (2022).